Bioinspiration & Biomimetics



RECEIVED 22 June 2021

REVISED

27 August 2021

ACCEPTED FOR PUBLICATION 9 September 2021

PUBLISHED 15 October 2021 PAPER

A remotely controlled Marangoni surfer

Mitchel L. Timm¹, Saeed Jafari Kang¹, Jonathan P. Rothstein² and Hassan Masoud^{1,*}

- Department of Mechanical Engineering-Engineering Mechanics, Michigan Technological University, Houghton, MI 49931, United States of America
- ² Department of Mechanical and Industrial Engineering, University of Massachusetts, Amherst, MA 01003, United States of America
- * Author to whom any correspondence should be addressed.

E-mail: hmasoud@mtu.edu

Keywords: Marangoni effect, surfing robot, remotely controlled, self-powered Supplementary material for this article is available online

Abstract

Inspired by creatures that have naturally mastered locomotion on the air—water interface, we developed and built a self-powered, remotely controlled surfing robot capable of traversing this boundary by harnessing surface tension modification for both propulsion and steering through a controlled release of isopropyl alcohol. In this process, we devised and implemented novel release valve and steering mechanisms culminating in a surfer with distinct capabilities. Our robot measures about 110 mm in length and can travel as fast as 0.8 body length per second. Interestingly, we found that the linear speed of the robot follows a 1/3 power law with the release rate of the propellant. Additional maneuverability tests also revealed that the robot is able to withstand 20 mm s⁻² in centripetal acceleration while turning. Here, we thoroughly discuss the design, development, performance, overall capabilities, and ultimate limitations of our robotic surfer.

1. Introduction

Many biological organisms such as insects, arachnids, and even bacteria have the ability to stand upon the liquid surface of lakes and ponds by taking advantage of surface tension [1-11]. However, among these, a few have the unique ability to manipulate the surface tension force to also propel themselves across the liquid surface with a great speed and maneuverability. For instance, by releasing lipid-laden excretions (see figure 1(a)), certain insects can change the local surface tension (in this case lowering it, like adding dish soap to water), thereby causing a surface tension imbalance that pulls the insect in a forward direction. This phenomenon is known as Marangoni propulsion [9, 12–15] and is a method of generating thrust via creating surface tension gradients. The superb capability of these organisms to travel atop free surfaces is ripe for robotic applications [16, 17]. Indeed, from mechanically driven robotic systems designed to walk and jump across the water-air interface [18–26] to chemically driven surfers relying on Marangoni propulsion for mobility [27-43], researchers have been attempting to develop surface dwelling robots that mimic the locomotion of anthropods for decades.

However, a close inspection of the literature (especially on Marangoni surfers) reveals that the vast majority of the designed robots are rudimentary, in that either they are self-powered, but move in an uncontrolled fashion, or are powered and actively controlled through external means. Examples of the former include the so-called 'soap boat' [41], 'cocktail boat' [29], and other similar designs [28, 30, 32, 35, 36, 38–40, 44–47] that have been around since the time of Rayleigh [27]. Recent studies using thermocapillary action to initiate Marangoni propulsion [42, 48] are examples of the latter, where objects at the interface are remotely manipulated through the use of externally powered lasers. An exception among the robots designed to date are the Marangoni surfers of Kwak et al [33, 34, 37], which include remote steering capabilities (both active and passive) and are selfpowered. However, even these designs have notable limitations, such as a lack of active directional and/or speed control.

To address these technological deficiencies, we developed and built a self-powered surfing robot (see figure 1(b)) that stands atop the free surface of water and uses Marangoni propulsion, through a controlled release of isopropyl alcohol (IPA), for locomotion

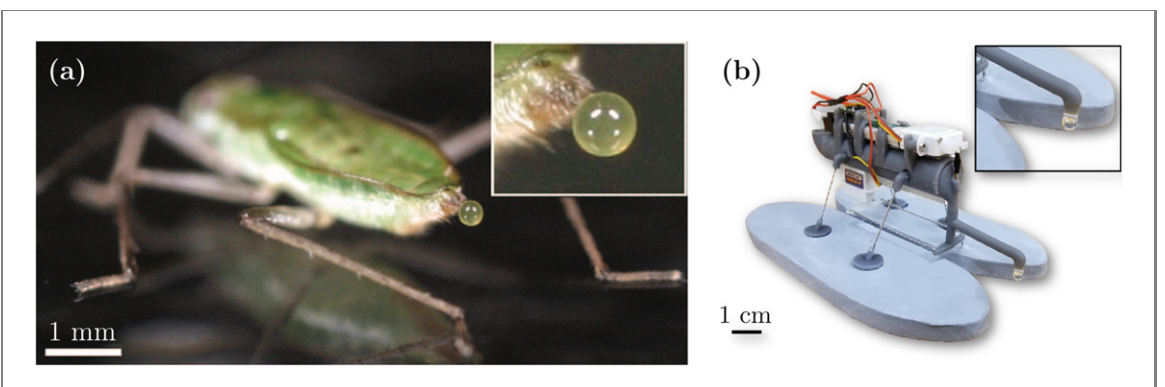


Figure 1. (a) *Mesovelia* secreting a drop of lipid-laden liquid waste. Reprinted from [12], Copyright (2007), with permission from Elsevier. (b) Our surfing robot inspired by the use of Marangoni propulsion among insects.

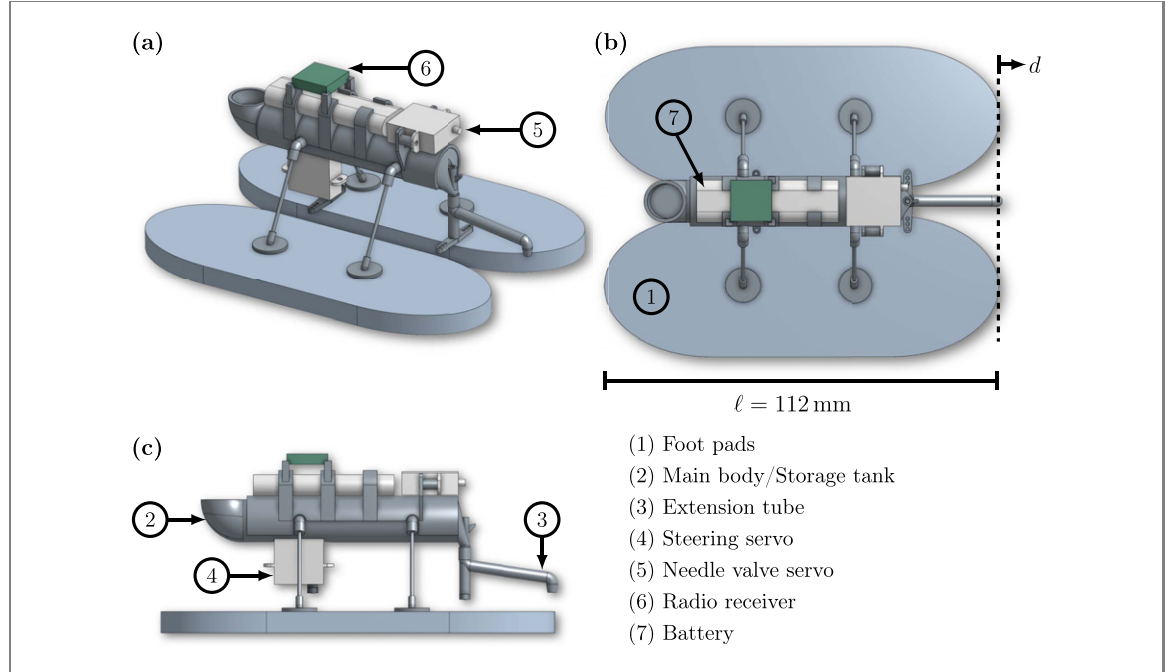


Figure 2. CAD model of the full robot assembly (shown in (a) isometric, (b) top, and (c) side views) along with the annotated list of its main components. See also figure 3 and video 1 of SM.

and maneuvering, while having the additional capability of being remotely controlled in both direction and speed. These features were achieved by devising a needle valve and a swiveling extension tube (both custom-made) that control the release rate and location of IPA, respectively. These mechanisms are powered by a pair of remotely controlled servos and are responsible for adjusting the speed and orientation of the surfer. As an added benefit of these methods for directional and speed control, there are no noisy engines or propellers in our design, making it virtually silent in operation. Also, fewer disturbances are introduced into the bulk of the liquid, thereby reducing the drag and making the robot more alike to the insects whose propulsion behavior it strives to mimic. With these attributes, our Marangoni surfer is ideal for a variety of practical applications. For example, with the simple addition of a small camera, it can easily be used by biologists, nature photographers, and wildlife experts to get up close to hard to reach aquatic locations and even skittish wildlife for photography or videography. This technology can also be used to monitor for invasive species in or near bodies of water. Lastly, with the silent and small nature of our robot, this design is a perfect candidate for surveillance in or near aquatic locations. In the following sections, we will first describe the design, development, and fabrication of the robot (section 2). Then, we will present the results of the performance tests, discuss the implications (section 3), and, finally, provide a brief summary of our work (section 4).

2. Design and fabrication of the robot

From insects such as *Mesovelia* (see figure 1(a)), we identified four distinct features, which we adopted and built into the design of our robot, that make for a successful remotely controlled surfer. These characteristics include the flotation of the robot on the water–air interface via surface tension, using

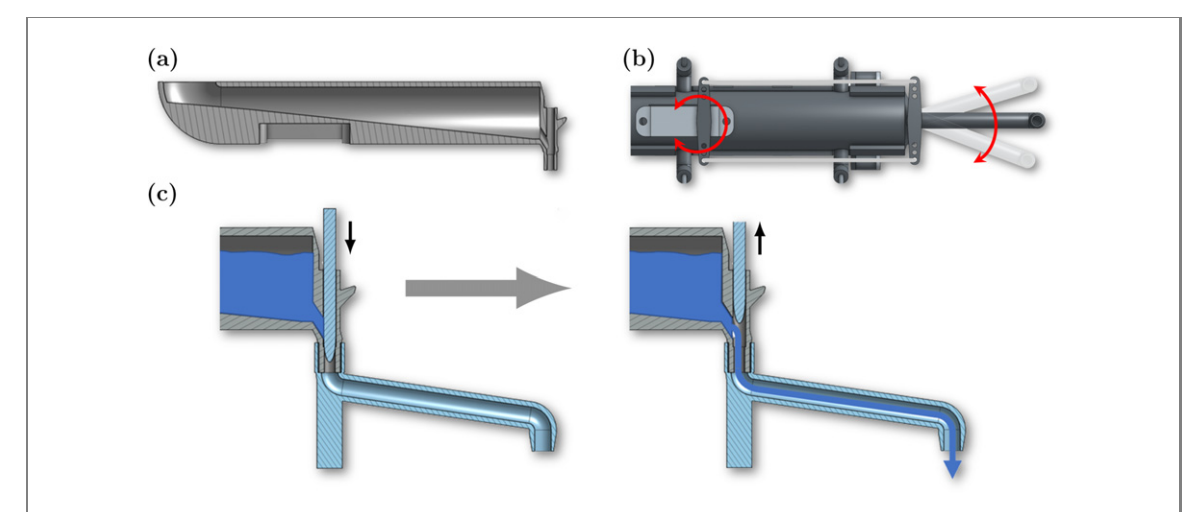


Figure 3. Diagrams depicting the internal structures and/or machinery of (a) the fuel tank/body, (b) the steering mechanism, and (c) the needle valve. See also video 1 of SM.

Marangoni propulsion as a primary means of locomotion, having an integrated power source (i.e. being self-powered), and the ability of actively controlling both speed and direction. These traits were integrated into our robotic surfer through the specific design and application of the foot-pads, propellant release mechanism, integrated battery and fuel sources, and remotely controlled servos, respectively (see figures 1(b) and 2, and video 1 of (https://stacks.iop.org/BB/16/066014/mmedia) supplementary materials (SM)). The development of the aforementioned components are described below.

Foot - **pads**. The feet are the point of contact with the liquid surface and are essential components to make our robot a functional surfer. They were designed with the objective of providing maximum support force from the surface tension while minimizing the hydrodynamic drag and mass. We first employed a simple force balance to estimate the surface contact perimeter necessary to support the weight of the surfer body (19 g, not including the footpads) plus the weight of fuel (3.14 g for 4 ml of IPA) [10]. Informed by this analysis, we made two separate ski-like foot pads (see figure 2 and video 1 of SM) in the form of elongated ellipses (112 mm by 40 mm) to serve our initial goals while maintaining the bioinspired design. In nature, the supporting force most anthropods use to stand upon free surfaces is achieved from the microscopic hairs on their feet and legs which trap tiny air pockets thereby increasing their hydrophobicity [12, 49, 50]. To adopt this quality to our design, we coated the feet with a commercially available hydrophobic treatment (NeverWet), allowing for greater support from surface tension (\sim 78 g total) due to the increase in contact angle with the free surface of water. The feet were made from 6 mm thick ethylene-vinyl acetate foam, which serves a dual purpose by being both light weight and highly buoyant. This way, if the robot were to hit an obstruction, it

would not sink (like previous attempts reported elsewhere), which could destroy the on-board electronics.

Fuel tank/body. The body of the surfer not only serves as the central base structure connecting the feet, servos, battery, radio receiver, and control mechanisms, but also acts as a storage vessel for the chemical propellant (in this case IPA, which is chosen for its ease of use, availability, and ubiquity). With the main body being a hollow cylindrical tank (3D-printed using Formlabs' standard grey resin), we eliminated any unnecessary connective structures, thereby reducing non-essential weight as much as possible. The tank is completely open at the front to avoid flow restrictions from a vacuum, and the needle valve and extension tube mechanisms are directly attached to the rear end of the tank (see figure 2 and video 1 of SM). At its current capacity, the tank can store 4 ml of chemical propellant. However, this design can be easily adjusted to accommodate higher volumes if required. To allow gravity to drive a relatively steady release of IPA (especially at low volumes), a sloped structure was designed into the horizontal tank (see figure 3(a)). This feature, while adding to the total weight, keeps the overall mass distribution along the robot fairly uniform.

Needle valve. The controlled release of the propellant has been attempted in previous Marangoni surfer designs. However, most have relied on passive means of control, i.e. calibrating a desired release rate and holding it constant [33, 34, 37]. Our design, on the other hand, has the ability of actively controlling the release rate of the propellant remotely through the novel implementation of a custom-created needle valve at the point of release (see figure 3(c) and video 1 of SM). Controlled by a remotely-operated servo, the position of the needle can be manipulated to block or restrict the flow of propellant to achieve the desired flow rate, which, in turn, adjusts the speed of the robotic surfer.

Steering mechanism. Steerablity is another distinguishing feature that separates surfers today from the time of Rayleigh, yet, the amount of progress that has been made is an indication of the difficulty of realizing this capability. Previously considered mechanisms for the directional manipulation of surfers (be it passive keels [37], actively controlled oars [33], or externally powered lasers [42, 48]), though functional, lack active control, are not self-powered, or adversely affect the surfing performance by introducing additional drag. Our surfer utilizes Marangoni propulsion not only as a mode of locomotion, but for steering as well, which eliminates unnecessary drag while maintaining the self-powered nature of the design. The steering mechanism operates by altering the bilateral release location of the propellant (see figure 3(b) and video 1 of SM), causing asymmetrical applied forces on the two foot-pads, which results in a change in the direction. The mechanism is driven by an actively controlled servo that is rigidly connected to the extension tube, which is a separate component from the main body and directly connects to the rear of the robot (see figure 2(b)). The steering mechanism allows for the extension tube to swivel and relocate the point at which the propellant is released (see figure 3(c) and video 1 of SM).

Remote controls. The remote control of both speed and direction is a critical feature of this robot for it to be of practical use. To achieve this, we implemented a micro-receiver (OrangeRx R614XN) and a remote transmitter (Spektrum DX7s) traditionally used for remotely controlled planes, cars, and boats (see figure 1(b) and video 1 of SM). With this receiver, we are able to simultaneously connect to two microservo motors (HobbyKing HK-5320s) achieving the ability to control both functionalities and power them with a small on-board battery (Turnigy Nano-Tech 150 mAh1S3.7 V25C LiPoly). Although others have utilized similar technology to remotely control their robotic surfers [33, 34], none have had the combined capabilities of our design.

3. Performance of the robot

To assess the overall capabilities of our Marangoni robot and to identify its optimal configuration, we performed two sets of experiments focusing on the translational speed and maneuverability of the surfer. Having already calculated and confirmed the proper size of foot-pads, we first characterized how fast the robot travels as a function of two parameters: the release rate of IPA (denoted by q) and the distance from the release site to the back of the foot-pads (denote by d, see figure 2(b)). Then, we examined the obstacle avoidance capability of the robot. All experiments were performed in an open-air cylindrical tank of diameter 1.47 m filled with 0.4 m-deep water.

For the speed tests, we captured the motion of the Marangoni surfer on video while traveling in a straight line for various values of the IPA release rate, q and release location d (see figure 4(a)). The speed was then extracted from the recorded data (see, e.g. video 2 of SM) using video analysis software (Tracker) in combination with a linear scale floated on the surface of the water during the tests for reference (see figure 4(a) and video 2 of SM). The release rate of IPA was adjusted by setting the controls of the transmitter to discrete position marks, thereby changing the relative position of the needle valve and the corresponding flow rate. The precise volumetric flow rate for each setting was measured prior to the experiments to ensure the accuracy and consistency of each test. The release distance was altered by using extension tubes (see figure 2) of different lengths. The results of the speed tests are presented in figure 5(a), with the speed (denoted by U) described in both mms⁻¹ and ℓ/s , where $\ell = 112$ mm is the body length of the robot shown in figure 2(b). The IPA flow rates that were tested range from 0.02 to 0.15 mls⁻¹, while the release distance was initially set to d = 0 and then increased in 5 mm increments to a maximum of d = 20 mm. Negative values of d were not considered due to the lack of sufficient lateral stability and the tendency to spin even without active steering.

Before we discuss the trends of data, for reference, we compare the speed of our robot to those of Kwak and Bae [33, 37] that are closest in functionality and form to ours. Their first Marangoni surfer [33] had remote steering capabilities, while also being similar in scale to our robot (~ 100 mm in length and ~ 20 g in mass). Opting instead to use methanol as a propellant, they were able to achieve a speed of 35 mms⁻¹ at a release rate of ~ 0.167 mls⁻¹. A later revision of their design [37] had a reduced mass of 11 g by eliminating the steering mechanisms and associated electronic components. After these alterations, their surfer was able to travel $\sim 90 \text{ mms}^{-1}$ with a release rate of $\sim 0.038 \text{ mls}^{-1}$. From a comparison to these works representing the state-of-theart in robotic Marangoni surfers, we can see that our robot is highly competitive, if not superior, in both performance and function. With this in mind, we now analyze the results of figure 5(a). First, we see that the speed of the surfer increases with the rate of IPA release, whereas it decreases with increased distance of release. Within the parameter space we evaluated, the surfer speed is in fact more sensitive to the release distance than the IPA release rate. We also observe that the relation between the surfer speed and the IPA release rate follows a power law such that $\mathcal{U} \propto q^{1/3}$ as shown by the dashed line in figure 5(a).

In order to rationalize the observed power law behavior, we propose a simple scaling analysis based on an energy argument. Let $\text{Re} = \mathcal{U}\ell/\nu$ be the flow Reynolds number, where ν is the kinematic viscosity of water. This dimensionless parameter measures the relative strength of inertial and viscous forces exerted on the surfer by the fluid. In our experiments, the

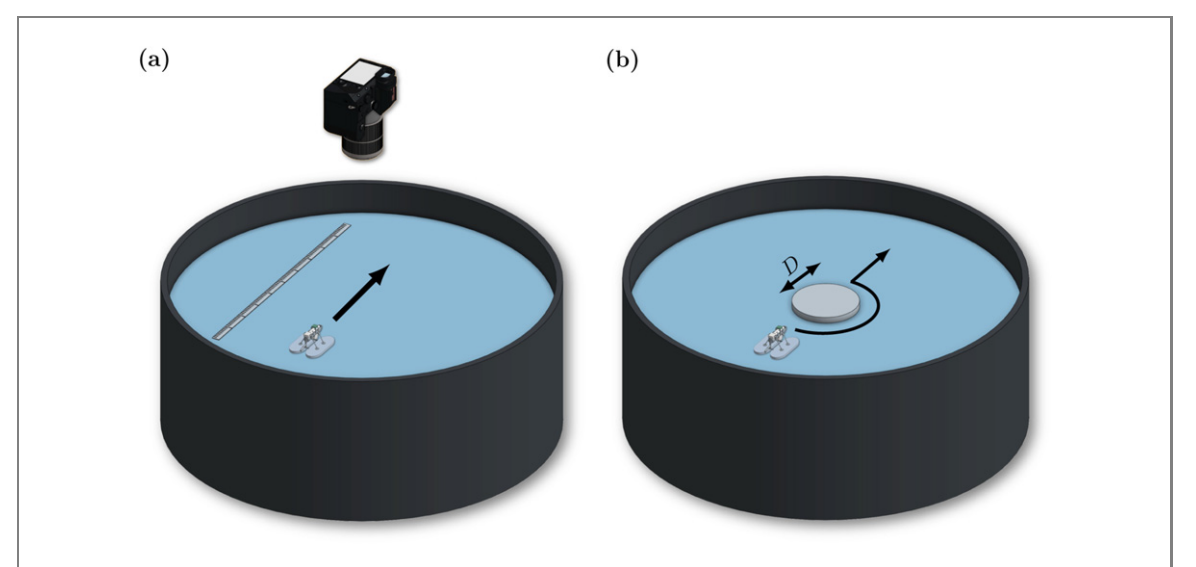


Figure 4. Schematics of the experimental setups used for (a) speed and (b) obstacle avoidance tests. See also videos 2 and 3 of SM.

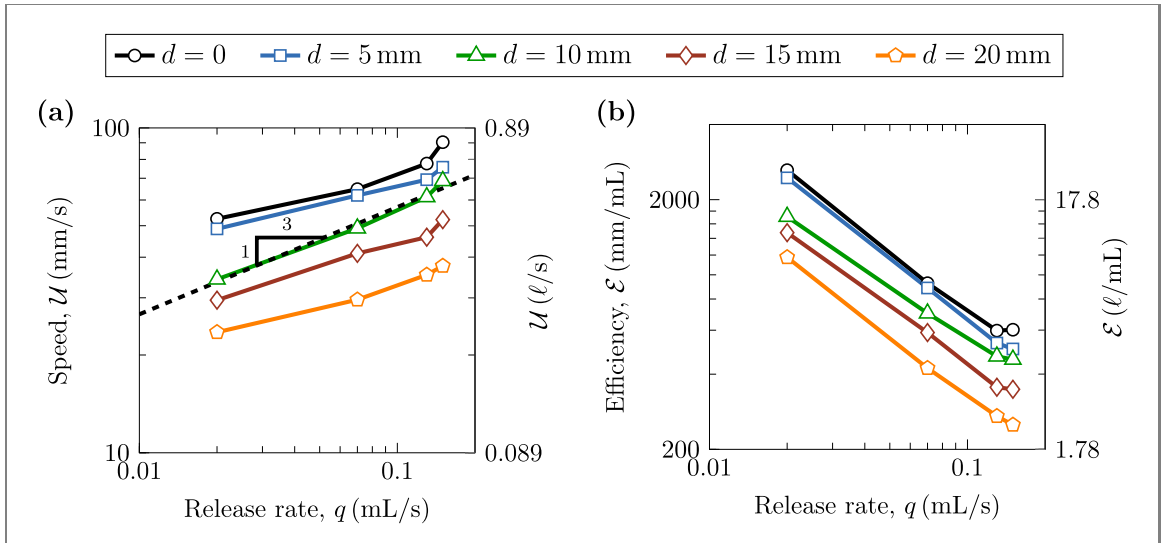


Figure 5. Plots of (a) the linear speed \mathcal{U} and (b) the fuel efficiency \mathcal{E} versus the release rate of the chemical propellant q for different values of the release distance d (see figure 2(b)). The predictions of a simple model is presented in (a) as a dashed line of slope 1/3.

Reynolds number is of order Re $\sim \mathcal{O}(10^3-10^4)$. This means that the robot operates in the inertial regime, where the fluid drag on the surfer primarily scales as $F_{\rm drag} \propto \mathcal{U}^2$. The power needed to maintain motion while overcoming a constant drag force is given by $P = \mathcal{U}F_{\text{drag}}$. Thus, the power to propel the surfer across the surface of the water at a speed $\mathcal U$ should scale like $P \propto \mathcal{U}^3$. In our design, the driving power comes from the release of chemical energy through lowering the air-water surface tension behind the surfer. The driving power should therefore change roughly linearly with the release rate of IPA, i.e. $P \propto q$. From our analysis, it is therefore expected that the surfer velocity should vary with the release rate to the power of 1/3, i.e. $\mathcal{U} \propto q^{1/3}$. This is confirmed by the quality of the fit of this scaling argument to the data in figure 5(a). One implication of these results is that the speed of the surfer is not particularly sensitive to the release rate, with the result being only a 30% change in velocity over an order of magnitude change in the release rate. In order to obtain improved control, future robot designs will include a needle valve that can provide periodic IPA release to reduce the minimum release rate that can be achieved and expand the lower range of surfer speeds that can be obtained.

To gain additional insights into the performance characteristics of our robot, we also calculated the fuel efficiency of the surfer. Here, the fuel efficiency is defined as $\mathcal{E} = \mathcal{U}/q$, and plotted versus the IPA release rate in figure 5(b). Unlike the robot speed, the fuel efficiency is highly sensitive to the rate at which IPA is discharged, and a negative trend in fuel efficiency is observed with increasing the IPA release rate with nearly an order of magnitude drop in efficiency over the range of release rates studied here. These results

Table 1. Results of obstacle avoidance tests for $d=10\,$ mm, where centripetal accelerations corresponding to successful and failed attempts are colored green and red, respectively.

		D			Centripetal acceleration (mm s ⁻²)		
$q(\text{mm s}^{\text{-}1})$	$\mathcal{U}\left(\mathrm{mms}^{\text{-}1} ight)$	ℓ	2ℓ	3ℓ	$2\mathcal{U}^2/\ell$	\mathcal{U}^2/ℓ	$2\mathcal{U}^2/3\ell$
0.02	34.2	\checkmark	\checkmark	\checkmark	20.9	10.4	7.0
0.07	49.1	×	\checkmark	\checkmark	43.1	21.5	14.4
0.13	61.3	×	×	✓	67.1	33.6	22.4

demonstrate that the most efficient operation of the robot surfer occurs at its lowest speeds. This makes intuitive sense, as the scaling analysis described above suggests that the efficiency should scale as $\mathcal{E} \propto q^{-2/3}$. This scaling is consistent with the data in figure 5(b).

The maneuverability tests were conducted by introducing a floating obstacle of diameter D for the surfer to avoid (see figure 4(b) and video 3 of SM). The obstacle was placed in the middle of the tank and anchored to its bottom via a wire cable under tension, ensuring the obstacle remained stationary despite the close proximity of flow disturbances due to the motion of the surfer. The robot was initially set on a straight path and then manually steered to bypass the obstacle. Steering was initiated approximately D/2 before reaching the obstacle. Following the contour of the obstacle as closely as possible, the surfer then continued on its initial path after reaching the far side of the obstacle (see figure 4(b) and video 3 of SM). If the surfer collided with the obstacle or spun out of control during the attempt, then the maneuver was considered a failure. For a given release rate, and therefore a given translational speed, this process was repeated until an obstacle of sufficiently large diameter was found, from which avoidance was possible. This set of tests were carried out for the fixed release distance of d = 10 mm, which offers a reasonable trade-off between speed and ease of steering. While smaller release distances produce higher speeds, they are also more difficult to steer. Contrarily, larger release distances, though slower, are less prone to abrupt changes in direction.

The outcome of the maneuverability tests are presented in table 1. Here, we examined the ability of the robot to avoid disks of diameter $D = \ell$, 2ℓ , and 3ℓ at the speeds $\mathcal{U} = 34.2$, 49.1, and 61.3 mms⁻¹. For each diameter-speed combination, a check mark in the table indicates that the robot was able to successfully go around the disk while a cross denotes failure to accomplish the mission. Similar to terrestrial vehicles, we found that the slower the traveling speed, the smaller turning radius the surfer could achieve. Specifically, the measurements suggest that the maximum centripetal acceleration achievable by the surfer under stable conditions is about 20 mms⁻²

(see the boxed values in table 1). Of course, these tests were conducted while traveling at *constant* speeds, and although the data show the inability of the surfer to make turns with small radii ($D \lesssim 3\ell$) at higher speeds, if one were to slow down when turning and speed up when going straight, this issue would be much reduced. Nevertheless, we note that the turning capability of our robot far exceeds that of its closest peer [33], whose turning radius (according to the reported measurements) is about five times larger than that of our robotic surfer at similar speeds.

4. Conclusion

Drawing motivation from organisms that effectively traverse the air-water interface, we conceptualized and created a self-powered and remotely-controlled robotic platform destined for practical applications. Prioritizing drag reduction and biomimicry in design, our robotic surfer relies solely on the Marangoni effect for both propulsion and change of direction. To make this engineering challenge a reality, we developed custom-made flow control and steering mechanisms. These features were complemented with integrated power and fuel sources, and a remote transmitter, a receiver, and two servos, overall resulting in a non-tethered robotic surfer with unparalleled functionality. From experimental trials investigating the robot's transnational motion, we found that there is a clear positive trend in the speed with increasing the release rate of the propellant. We then presented a scaling analysis justifying the observed power law relationship between the speed and the consumption rate of the chemical fuel. We also examined the range of maneuverability of our robot, and demonstrated its commendable capabilities for directional change and obstacle avoidance.

Through assessing the combined abilities and promising performance of our surfing robot, we gained a glimpse of its enormous potential. Specifically, our robot serves as a desirable candidate for accomplishing complicated missions at the free surface of water, where the precise remote-control of position and speed is essential. A prime example that would require minimal modification to our current

design is the directed self-assembly of objects, particles, or even organisms (such as bacteria or cells) at the air-water interface. This process has been at the center of scientists' attention for decades [51-54], with implications ranging from advanced manufacturing to medicine. Our robot presents a viable solution to this long-lived conundrum (see, e.g. [42]). In addition to the currently tangible goal of directed selfassembly, a more ambitious, yet achievable aspiration is to make our robot autonomous. With the addition of an inertial measurement unit coupled with a small camera as an optical sensor, the robot could be trained to identify targets, markers, and obstacles and automatically adjust its trajectory in accordance with its designated task. Through autonomy, the robot could perform the same tasks previously described while also being able to optimize its movements.

Acknowledgments

Financial support from the National Science Foundation under Grant Nos. CBET-1749634 (HM) and CBET-1705519 (JPR) is acknowledged.

Data availability statement

All data that support the findings of this study are included within the article (and any supplementary files).

ORCID iDs

Jonathan P. Rothstein https://orcid.org/0000-0002-9344-1133

Hassan Masoud b https://orcid.org/0000-0001-8932-3479

References

- [1] Miyamoto S 1955 On a special mode of locomotion utilizing surface tension at the water-edge in some semiaquatic insects *Kontyu* 23 45–52
- [2] Nachtigall W 1974 Locomotion: Mechanics and Hydrodynamics of Swimming in Aquatic Insects (New York: Academic) pp 381–432
- [3] Andersen N M 1976 A comparative study of locomotion on the water surface in semiaquatic bugs (insects, Hemiptera, Gerromorpha) Vidensk. Meddr. Dansk Naturh. 139 337–96
- [4] Suter R, Rosenberg O, Loeb S, Wildman H and Long J 1997 Locomotion on the water surface: propulsive mechanisms of the Fisher spider J. Exp. Biol. 200 2523–38
- [5] Bowdan E 1978 Walking and rowing in the water strider, Gerris remigis J. Comp. Physiol. 123 43-9
- [6] Suter R B and Wildman H 1999 Locomotion on the water surface: hydrodynamic constraints on rowing velocity require a gait change J. Exp. Biol. 202 2771–85
- [7] Betz O 2002 Performance and adaptive value of tarsal morphology in rove beetles of the genus Stenus(Coleoptera, Staphylinidae) J. Exp. Biol. 205 1097–113

- [8] Stratton G E, Suter R B and Miller P R 2004 Evolution of water surface locomotion by spiders: a comparative approach *Biol. J. Linn. Soc.* 81 63–78
- [9] Bush J W M and Hu D L 2006 Walking on water: biolocomotion at the interface *Annu. Rev. Fluid Mech.* 38 339–69
- [10] Hu D L and Bush J W M 2010 The hydrodynamics of water-walking arthropods J. Fluid Mech. 644 5–33
- [11] Lang C, Seifert K and Dettner K 2012 Skimming behaviour and spreading potential of Stenus species and *Dianous* coerulescens (Coleoptera: Staphylinidae) Naturwissenschaften 99 937–47
- [12] Bush J W M, Hu D L and Prakash M 2007 The integument of water-walking arthropods: form and function Adv. Insect Physiol. 34 117–92
- [13] Masoud H and Stone H A 2014 A reciprocal theorem for Marangoni propulsion J. Fluid Mech. 741 R4
- [14] Kang S J, Sur S, Rothstein J P and Masoud H 2020 Forward, reverse, and no motion of Marangoni surfers under confinement *Phys. Rev. Fluids* 5 084004
- [15] Vandadi V, Kang S J and Masoud H 2017 Reverse Marangoni surfing J. Fluid Mech. 811 612–21
- [16] Hu D L, Prakash M, Chan B and Bush J W M 2010 Water-walking Devices (Berlin: Springer) pp 131–40
- [17] Kwak B and Bae J 2018 Locomotion of arthropods in aquatic environment and their applications in robotics *Bioinspir. Biomim.* 13 041002
- [18] Song Y S and Sitti M 2007 Surface-tension-driven biologically inspired water strider robots: theory and experiments *IEEE Trans. Robot.* 23 578–89
- [19] Zhao J, Zhang X and Pan Q 2012 A water walking robot inspired by water strider 2012 IEEE Int. Conf. Mechatronics and Automation (IEEE) pp 962–7
- [20] Koh J-S, Jung S-p., Wood R J and Cho K-J 2013 A jumping robotic insect based on a torque reversal catapult mechanism 2013 IEEE/RSJ Int. Conf. Intelligent Robots and Systems (IEEE) pp 3796–801
- [21] Ozcan O, Wang H, Taylor J D and Sitti M 2014 STRIDE II: a water strider-inspired miniature robot with circular footpads Int. J. Adv. Rob. Syst. 11 85
- [22] Koh J-S and Cho K-j 2014 Development of an insect size micro jumping robot Conf. Biomimetic and Biohybrid Systems (Springer) pp 405–7
- [23] Koh J-S et al 2015 Jumping on water: surface tension-dominated jumping of water striders and robotic insects Science 349 517–21
- [24] Yang K, Liu G, Yan J, Wang T, Zhang X and Zhao J 2016 A water-walking robot mimicking the jumping abilities of water striders *Bioinspir*. *Biomim*. 11 066002
- [25] Sun J, Li X, Song J, Huang L, Liu X, Liu J, Zhang Z and Zhao C 2018 Water strider-inspired design of a water walking robot using superhydrophobic Al surface J. Dispersion Sci. Technol. 39 1840–7
- [26] Chukewad Y M, James J, Singh A and Fuller S 2021 Robofly: an insect-sized robot with simplified fabrication that is capable of flight, ground, and water surface locomotion IEEE Trans. Robot. 1–16
- [27] Rayleigh L 1889 Measurements of the amount of oil necessary in order to check the motions of camphor upon water Proc. R. Soc. 47 364–7
- [28] Su M 2007 Liquid mixing driven motions of floating macroscopic objects Appl. Phys. Lett. 90 144102
- [29] Burton L J, Cheng N and Bush J W 2014 The cocktail boat Integr. Comp. Biol. 54 969–73
- [30] Musin A, Grynyov R, Frenkel M and Bormashenko E 2016 Self-propulsion of a metallic superoleophobic micro-boat J. Colloid Interface Sci. 479 182–8
- [31] Akella V S, Singh D K, Mandre S and Bandi M M 2018 Dynamics of a camphoric acid boat at the air–water interface *Phys. Lett.* A 382 1176–80
- [32] Zhang L, Yuan Y, Qiu X, Zhang T, Chen Q and Huang X 2017 Marangoni effect-driven motion of miniature robots

- and generation of electricity on water *Langmuir* **33** 12609–15
- [33] Kwak B and Bae J 2017 Skimming and steering of a non-tethered miniature robot on the water surface using Marangoni propulsion 2017 IEEE/RSJ Int. Conf. Intelligent Robots and Systems (IROS) pp 3217–22
- [34] Kwak B, Lee D and Bae J 2018 Flexural joints for improved linear motion of a Marangoni propulsion robot: design and experiment 2018 7th IEEE Int. Conf. Biomedical Robotics and Biomechatronics (Biorob) pp 1321–6
- [35] Zhang H, Duan W, Liu L and Sen A 2013 Depolymerization-powered autonomous motors using biocompatible fuel J. Am. Chem. Soc. 135 15734–7
- [36] Sharma R, Chang S T and Velev O D 2012 Gel-based self-propelling particles get programmed to dance *Langmuir* 28 10128–35
- [37] Kwak B, Choi S and Bae J 2020 Directional motion on water surface with keel extruded footpads propelled by Marangoni effect *IEEE Robot. Autom. Lett.* 5 6829–36
- [38] Pena-Francesch A, Giltinan J and Sitti M 2019 Multifunctional and biodegradable self-propelled protein motors Nat. Commun. 10 1–10
- [39] Luo C, Li H, Qiao L and Liu X 2012 Development of surface tension-driven microboats and microflotillas *Microsyst*. *Technol.* 18 1525–41
- [40] Jin H, Marmur A, Ikkala O and Ras R H A 2012 Vapour-driven Marangoni propulsion: continuous, prolonged and tunable motion *Chem. Sci.* 3 2526–9
- [41] Renney C, Brewer A and Mooibroek T J 2013 Easy demonstration of the Marangoni effect by prolonged and directional motion: 'soap boat 2.0' J. Chem. Educ. 90 1353-7
- [42] Basualdo F N P, Bolopion A, Gauthier M and Lambert P 2021 A microrobotic platform actuated by thermocapillary flows for manipulation at the air—water interface *Sci. Robot.* 6 eabd3557

- [43] Choi Y et al 2021 Photopatterned microswimmers with programmable motion without external stimuli Nat. Commun. 12 1–8
- [44] Nakata S, Iguchi Y, Ose S, Kuboyama M, Ishii T and Yoshikawa K 1997 Self-rotation of a camphor scraping on water: new insight into the old problem *Langmuir* 13 4454–8
- [45] Kitahata H, Hiromatsu S-i, Doi Y, Nakata S and Rafiqul Islam M 2004 Self-motion of a camphor disk coupled with convection *Phys. Chem. Chem. Phys.* 6 2409–14
- [46] Soh S, Bishop K J M and Grzybowski B A 2008 Dynamic self-assembly in ensembles of camphor boats J. Phys. Chem. B 112 10848–53
- [47] Nakata S and Murakami M 2010 Self-motion of a camphor disk on an aqueous phase depending on the alkyl chain length of sulfate surfactants *Langmuir* 26 2414–7
- [48] Maggi C, Saglimbeni F, Dipalo M, De Angelis F and Di Leonardo R 2015 Micromotors with asymmetric shape that efficiently convert light into work by thermocapillary effects Nat. Commun. 6 1–5
- [49] Feng X-Q, Gao X, Wu Z, Jiang L and Zheng Q-S 2007 Superior water repellency of water strider legs with hierarchical structures: experiments and analysis *Langmuir* 23 4892–6
- [50] Prakash M and Bush J W M 2011 Interfacial propulsion by directional adhesion Int. J. Non-Linear Mech. 46 607–15
- [51] Bowden N, Terfort A, Carbeck J and Whitesides G M 1997 Self-assembly of mesoscale objects into ordered two-dimensional arrays Science 276 233-5
- [52] Mastrangeli M, Abbasi S, Varel C, Van Hoof C, Celis J-P and Böhringer K F 2009 Self-assembly from milli to nanoscales: methods and applications J. Micromech. Microeng. 19 083001
- [53] Grzelczak M, Vermant J, Furst E M and Liz-Marzán L M 2010 Directed self-assembly of nanoparticles ACS Nano 4 3591–605
- 54] Chen Q, Bae S C and Granick S 2011 Directed self-assembly of a colloidal kagome lattice *Nature* 469 381–4